RIGA TECHNICAL UNIVERSITY

Jingzhi Fan

METABOLITE INCORPORATION IN BIOMATERIALS FOR BONE TISSUE REGENERATION

Summary of the Doctoral Thesis

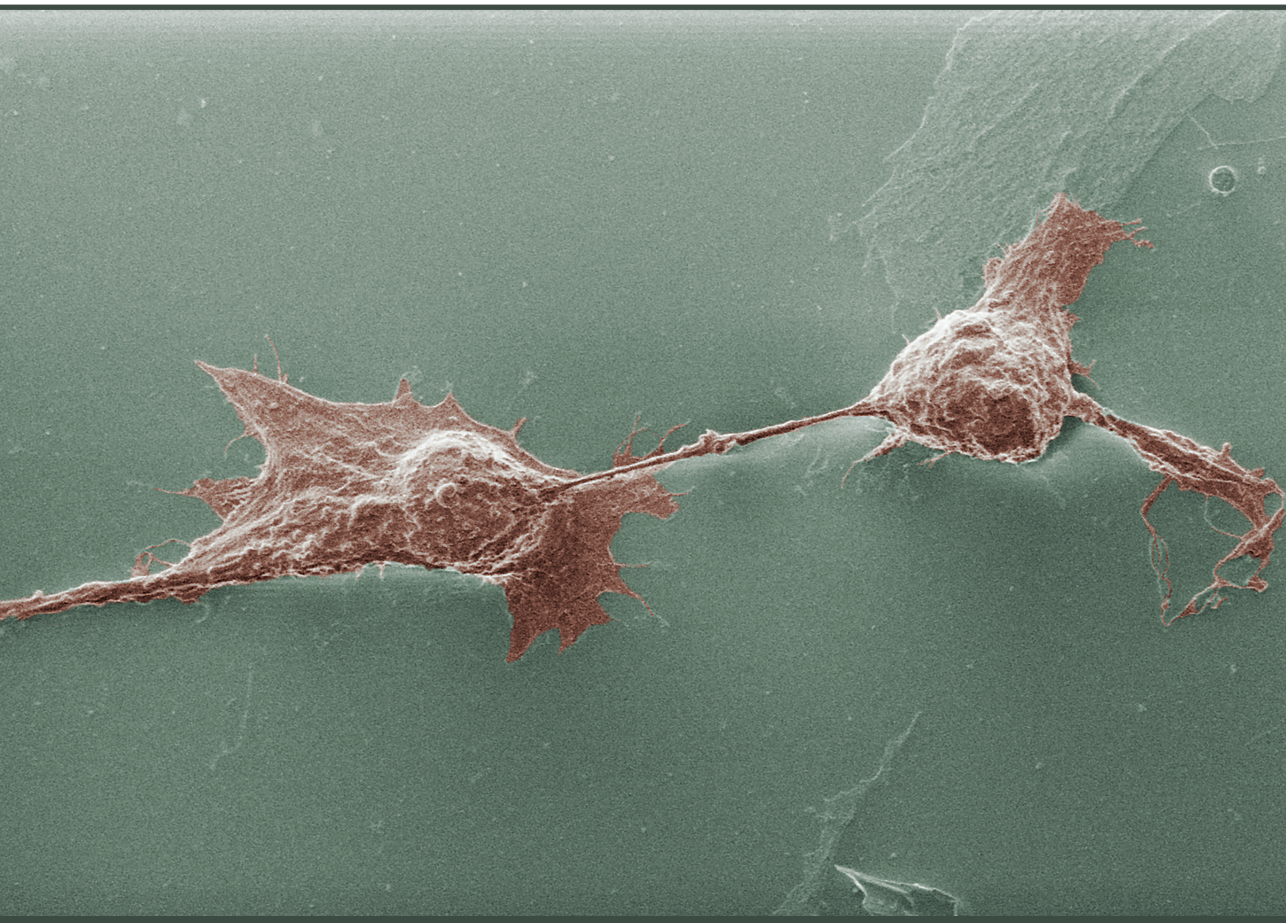

RTU Press
Riga 2025

RIGA TECHNICAL UNIVERSITY
Faculty of Natural Sciences and Technology
Institute of Biomaterials and Bioengineering

Jingzhi Fan
Doctoral Student of the Study Programme "Chemistry, Materials Science and Engineering"

METABOLITE INCORPORATION IN BIOMATERIALS FOR BONE TISSUE REGENERATION

Summary of the Doctoral Thesis

Scientific supervisors
Professor Dr. sc. ing.
DAGNIJA LOČA

Associate Professor Dr. nat. techn.
KRISTAPS KĻAVIŅŠ

RTU Press
Riga 2025

Fan, J. Metabolite Incorporation in Biomaterials for Bone Tissue Regeneration. Summary of the Doctoral Thesis. Riga: RTU Press, 2025. 28 p.

Published in accordance with the decision of the Promotion Council "RTU P-02" of 29 September 2025, Minutes No. 04030- 9.2/7.

Acknowledgements

I want to express my gratitude to Kristaps Kļaviņš for his guidance and support throughout my PhD journey and Dagnija Loča for her tutoring and supervision of my PhD dissertation. I am also thankful to Antons Sizovs and Sophie Verrier for their assistance with animal data and Abhishek Indurkar for his help with material synthesis. My appreciation extends to Ilijana Kovrlija, Kristaps Rubenis, Theresa Schiemer, and all the others who contributed to this work.

Finally, I am grateful to my parents for their constant support and to my friends for their companionship. I also acknowledge with respect the sacrifices of the experimental animals used in this study.

This research has been supported by the European Union's Horizon 2020 research and innovation program under grant agreement No. 857287 (BBCE).

Cover picture by Jingzhi Fan.

https://doi.org/10.7250/9789934372377

ISBN 978-9934-37-237-7 (pdf)

DOCTORAL THESIS PROPOSED TO RIGA TECHNICAL UNIVERSITY FOR PROMOTION TO THE SCIENTIFIC DEGREE OF DOCTOR OF SCIENCE

To be granted the scientific degree of Doctor of Science (PhD), the present Doctoral Thesis has been submitted for defence at the open meeting of the RTU Promotion Council on 12th December 2025 at 14:00, at the Faculty of Natural Sciences and Technology of Riga Technical University, Paula Valdena iela 3, Room 272.

OFFICIAL REVIEWERS
Professor Dr. chem. Māris Turks
Riga Technical University

Associate Professor Dr. sc. ing. Egils Stalidzāns
Rīga Stradiņš University, Latvia

Associate Professor Dr. Gernot Schabbauer
Medical University of Vienna, Austria

DECLARATION OF ACADEMIC INTEGRITY

I hereby declare that the Doctoral Thesis submitted for review to Riga Technical University for promotion to the scientific degree of Doctor of Science (PhD) is my own. I confirm that this Doctoral Thesis has not been submitted to any other university for promotion to a scientific degree.

Jingzhi Fan ……. (signature)
Date: ……

The Doctoral Thesis has been written in English. It consists of an Introduction, four chapters, Conclusions, 58 figures, four tables, and one appendix; the total number of pages is 184, including the appendixes. The Bibliography contains 167 titles.

ANNOTATION

Metabolism plays a critical role in bone homeostasis, regeneration, and healing. This study explores the potential of biomaterials to modulate metabolic processes during bone healing as a clinically relevant strategy for biomaterial development. To this end, metabolic changes occurring during bone regeneration were characterized, and the findings were applied to tissue engineering strategies.

Metabolomic profiling was performed using samples from rat calvarial critical-sized defects and sheep tibial defect animal models to better understand systemic metabolic changes during bone regeneration. The results revealed that glutamate and glutamine were significantly downregulated during the healing process. Given the widespread use of calcium phosphate-based biomaterials as bone fillers in tissue engineering, the interaction between cells and materials was investigated using fibroblast cell lines exposed to various calcium phosphate compounds. The findings demonstrated that ceramic biomaterials can adsorb a broad range of small molecules from their microenvironment. Additionally, exposure to calcium phosphate-based materials influenced cellular amino acid levels and energy metabolism.

A novel amorphous calcium phosphate material synthesized from a glutamate source (ACP-Glu) was developed based on the insights from the critical-sized defect models. This new biomaterial was extensively characterized through osteogenesis and metabolomics studies. ACP-Glu exhibited superior performance in enhancing cellular energy metabolism and promoting osteogenic activity. The increased energy metabolism, particularly the tricarboxylic acid cycle, appeared to compensate for anaerobic glycolysis, providing the necessary energy to support tissue repair. As a result, ACP-Glu shows promise as a biomaterial for bone regeneration, potentially accelerating the healing process by promoting more efficient in situ energy metabolism.

This material could replace biologically inactive bone fillers, enhancing regenerative outcomes. Moreover, utilizing endogenous metabolites to modulate biological responses offers a safer alternative to bioactive additives such as cytokines and growth factors. The key practical contribution of this study is the development of ACP-Glu, which could assist patients with bone defects by accelerating hard tissue repair through replenishing depleted nutrients. The biomaterial design and evaluation methodology, particularly the metabolomic approaches employed in this research, could serve as a valuable reference for future work in the field.

Table of Contents

Abbreviations 6

Aims and objectives 7

Scientific novelty and main results 7

Practical application of the work 7

Work approval and publications as first author 8

Background 10

Metabolic changes during bone healing in animal models 11

Metabolomic investigation of cell-material interaction 13

The influence of exposure time and material composition on metabolism 15

The development of amorphous calcium phosphate with glutamate 15

Synthesis and manufacture of ACP-Glu 15

Characterization of ACP-Glu 16

Glutamate release characterization of ACP-Glu 17

Metabolomics investigation of cells on ACP-Glu 18

Differential Metabolite Profiles of ACP-Glu and Control Groups 18

Metabolite difference between ACP-Glu and ACP 19

Osteogenic Assessment of ACP-Glu In Vitro 21

Biocompatibility test 22

Extracellular and intracellular calcium and phosphate levels 22

Osteogenesis evaluation 24

Mineralization evaluation 25

Conclusions 26

References 27

Acknowledgements 29

Abbreviations

ACP – amorphous calcium phosphate

ACP-GLU – amorphous calcium phosphate with glutamate

ALP – alkaline phosphatase

ANOVA – one-way variance analysis

ATP – adenosine triphosphate

CaP – calcium phosphate

CCK-8 – Cell Counting Kit-8

CNT – control group

FBS – fetal bovine serum

Glu – glutamate

H58 – calcium phosphate with 58 % hydroxyapatite and 42 % beta-tricalcium phosphate

H95 – calcium phosphate with 95 % hydroxyapatite and 5 % beta-tricalcium phosphate

HAP – hydroxyapatite

LC – liquid chromatography

LDH – lactate dehydrogenase

MS – mass spectrometry

OCN – osteocalcin

OCP – octacalcium phosphate

OPN – osteopontin

PBS – phosphate-buffered saline

PCA – principal component analysis

SEM – scanning electron microscope

TCA – tricarboxylic acid (citric acid) cycle

XRD – X-ray diffraction analysis

β-TCP – beta-tricalcium phosphate

Aims and objectives

The research aimed to develop a novel CaP-based biomaterial with an incorporated metabolite that enhances bone regeneration.

To achieve the aim, the following main tasks were proposed during this research:

1. Characterize systemic metabolic alterations during bone regeneration utilizing *in vivo* models, elucidating the dynamic changes in metabolic profiles associated with the healing process.
2. Investigate and characterize alterations in cellular metabolism induced by biomaterial interactions, employing advanced metabolomics techniques to delineate the molecular mechanisms underlying these changes.
3. Identify and validate potential bioactive metabolites integral to bone healing, unraveling specific metabolite signatures indicative of enhanced regenerative processes.
4. Synthesize biomaterials incorporating identified metabolites as a novel system, establishing a link between metabolomic discoveries and material design for enhanced bioengineering applications.
5. Evaluate the synthesized metabolite-loaded biomaterials' *in vitro* performance and physical properties, employing rigorous characterization methods to ascertain their suitability for clinical translation and potential impact on therapeutic outcomes.

The following theses are proposed for defense:

1. Bone healing in mammals triggers systemic alterations in energy and amino acid metabolism.
2. Calcium phosphate (CaP)-based biomaterials change cellular metabolic microenvironment by enhancing glycolytic activity.
3. Metabolites depleted during bone healing can be integrated into biomaterials to facilitate bone regeneration.

Scientific novelty and main results

1. The progress of bone healing has been widely researched; however, the knowledge of small molecular changes during this process is still vague. The metabolomics profiling from rat calvaria and sheep tibia provided a deeper understanding of systemic metabolome changes during bone regeneration. Notably, serum concentrations of glutamate and glutamine were significantly reduced during bone healing, indicating increased metabolic demand for these amino acids.
2. Cell-material interaction studies in the bioengineering field have mainly ignored the role of endogenous metabolites. This study demonstrated that ceramic biomaterials can adsorb a broad

range of small molecules from their surrounding microenvironment. The results also show that exposure to CaP-based materials affects cellular amino acids and energy metabolism.

3. Utilizing the results from the critical size defect models, amorphous calcium phosphate synthesized from a glutamate source was prepared. The new biomaterial, ACP-Glu (amorphous calcium phosphate incorporating glutamate), was characterized through established osteogenesis assays and metabolomics studies. ACP-Glu behaved excellently in boosting cell energy metabolism and osteogenesis properties. Enhanced energy metabolism, particularly increased tricarboxylic acid (TCA) cycle activity, could compensate for anaerobic glycolysis and supply the energy required for tissue repair. This material could be used as a biomaterial for bone regeneration with a faster healing rate by triggering more efficient in situ energy metabolism.

Practical application of the work

The metabolomic evaluation of systemic metabolic changes during bone regeneration offers a valuable reference for various biomedical fields, including nutrition, clinical medicine, rehabilitation, and bioengineering. Biomaterials absorbing small molecules from their environment are crucial in material design, highlighting the importance of interactions between materials and the adsorbed molecules. This Thesis demonstrates how metabolomics, as a powerful research tool, can be applied to evaluate biomaterials used in tissue engineering. The newly developed biomaterial, ACP-Glu, has shown the ability to significantly enhance bone cell activity by regulating energy metabolism. This material can replace biologically inactive bone fillers and improve regeneration outcomes. Moreover, utilizing endogenous metabolites to modulate biological responses presents a safer alternative to other bioactive additives, such as cytokines and growth factors. The primary practical outcome of this Thesis is the development of ACP-Glu, which can aid patients with bone defects by accelerating hard tissue repair through replenishing depleted nutrients.

Work approval and publications (first author)

Journals

1. Fan, J., Jahed, V., Klavins, K. Metabolomics in bone research. Metabolites. Jul. 2021, 1; 11(7): 434.
2. Fan, J., Abedi-Dorcheh, K., Sadat Vaziri, A., Kazemi-Aghdam, F., Rafieyan, S., Sohrabinejad, M., Ghorbani, M., Rastegar Adib, F., Ghasemi, Z., Klavins, K., Jahed, V. A review of recent advances in natural polymer-based scaffolds for musculoskeletal tissue engineering. Polymers. May 20, 2022; 14(10): 2097.

3. Fan, J., Schiemer, T., Vaska, A., Jahed, V., Klavins, K. Cell via Cell Viability Assay Changes Cellular Metabolic Characteristics by Intervening with Glycolysis and Pentose Phosphate Pathway. Chemical Research in Toxicology. Jan. 2024, 8; 37(2): 208–211.
4. Fan, J., Schiemer, T., Steinberga, V., Vaska, A., Metlova, A., Sizovs, A., Locs, J., Klavins, K. Exploring the Impact of Calcium Phosphate Biomaterials on Cellular Metabolism. Heliyon. Nov. 2024, 30; 10(22): e39753.

Conferences

1. Fan J., Indukar, A., Vaska, A., Golubeva, D., Verrier, S., Sizovs, A., Locs, J., Klavins, K. Metabolomics-Inspired Biomaterials: Amorphous Calcium Phosphate with Targeted Metabolic Enhancement for Bone Repair, in: 21st Annual International Conference of the Metabolomics Society, 22-26, June, 2025, Prague, Czech Republic.
2. Fan, J., Indukar A., Vaska, A., Golubeva, D., Verrier, S., Sizovs, A., Locs, J., Klavins, K. Metabolomics-Inspired Biomaterials: Amorphous Calcium Phosphate with Targeted Metabolic Enhancement for Bone Repair, in: The Scandinavian Society for Biomaterials conference 2025, 6-9, May, 2025, Hameenlinna, Finland.
3. Fan, J., Indukar, A., Vaska, A., Golubeva, D., Verrier, S., Sizovs, A., Locs, J., Klavins, K. Development of Amorphous Calcium Phosphate with Incorporated Metabolites for Enhanced Bone Healing, 12th World Biomaterials Congress, 26-31, May, Daegu, South Korea.
4. Jingzhi, F., Jahed, V., Kaufmane, L. V., Vaska, A., Sizovs, A., Loca, L., Sadovska, L., Line, A., Kristaps, K. Unraveling the Molecular Mechanisms of Cytotoxicity Induced by Physically Crosslinked Hyaluronic Acid/Poly-L-Lysine Hydrogel, 12th World Biomaterials Congress, 26-31, May, Daegu, South Korea.
5. Jingzhi, F., Jahed, V., Kaufmane, L.V., Klavins, K., Exploring the mechanism of PLL/HA hydrogel cytotoxicity, Materials Science and Applied Chemistry, 6, October, 2023, Riga, Latvia.
6. Fan, J., Schiemer, T., Vaska, A., Klavins, K. Influence of cell viability assay on cellular metabolisms, Tissue Engineering and Regenerative Medicine International Society EU chapter, 28-31, March, June, 2023, Manchester, UK.
7. Fan, J., Schiemer, T., Sizovs, A., Locs, J., Klavins, K. Metabolomics investigation of biomaterial-cell interactions, in: The Scandinavian Society for Biomaterials Conference, 13-15, June, 2022, Jurmala, Latvia.
8. Fan, J., Schiemer, T., Sizovs, A., Locs, J., Klavins, K. Calcium phosphate-based biomaterials influence on cell metabolism, in: Tissue Engineering and Regenerative Medicine International Society EU chapter, 28, June-1, July, 2022, Krakow, Poland.

9. Fan, J., Schiemer, T., Sizovs, A., Locs, J., Klavins, K., Calcium Phosphates-Based Biomaterial Influence on Cell Metabolism, in: Nordic Metabolomics Conference, 6-9, September, 2022, Copenhagen, Denmark.

Background

In 2019, 178 million new fractures and 455 million cases of acute or long-term fracture symptoms were reported globally [1]. Artificial interventions for repairing hard tissue defects are critical for effectively treating patients and improving their quality of life. Today, bone tissue engineering is advancing rapidly, utilizing cutting-edge biomaterials, scaffold designs, and cell-based therapies to develop innovative bone regeneration and repair solutions. Calcium phosphate plays a crucial role in bone tissue engineering as it mimics the mineral composition of natural bone, promoting osteoconduction and osteoinduction [2]. Its biocompatibility allows for seamless integration with surrounding tissues, supporting bone regeneration and healing. Calcium phosphate-based scaffolds are widely used in tissue engineering to provide structural support and enhance cell attachment and proliferation, facilitating effective bone tissue regeneration [3]. Cold sintering, a novel processing technique, enables the consolidation of materials at significantly lower temperatures than traditional sintering methods, typically below 300 °C [4]. In the context of calcium phosphate, cold sintering offers a unique method for fabricating biocompatible scaffolds and implants with improved mechanical properties while preserving the chemical integrity of the material. This approach is especially advantageous for producing calcium phosphate-based biomaterials that incorporate bioactive small organic molecules for bone tissue engineering, as it reduces the risk of deactivating organic molecules and allows for better control over the final structure and properties of the implants.

Bone homeostasis is closely tied to metabolic processes, making metabolites valuable indicators for studying bone regeneration [5]. Metabolomics has been employed to identify potential biomarkers for diagnosing and prognosticating bone injuries [6], osteoporosis [7], and osteosarcoma [8]. Characterizing small molecular changes during bone regeneration can lead to the development of more efficient, personalized, and biomimetic tissue engineering solutions, contributing to improved healing outcomes and reduced complications in clinical practice [9].

This study leverages metabolomics technology in three key areas: 1) exploring hard tissue repair processes following bone defects *in vivo*, 2) understanding cell-material interactions at the molecular level, and 3) developing and characterizing novel materials.

Metabolic changes during bone healing in animal models

A critical-size calvarial defect model in rats was employed to evaluate metabolic changes during bone healing, a model recognized for its reliability and reproducibility in biomaterial assessment without the need for mechanical fixation. Calvarial defects, 8 mm in diameter, were created in male Wistar rats (8–12 weeks old) using trepanation. These defects constituted critical-size defects. Two groups were established for the study. In the first group ($n = 6$), the defect was left untreated (without repositioned calvaria group). In the second group ($n = 5$), the excised calvaria was cut into four pieces and repositioned in the defect site to promote healing (excised calvaria repositioned group). Blood samples were collected at three time points: before surgery, Day 1, and Day 3 – post-surgery. Metabolite extraction was performed using a methanol-based method, incorporating isotopically labeled internal standards. Targeted quantitative metabolite analysis was then performed using HILIC-based liquid chromatography, which enabled the quantification of 33 metabolites. The resulting metabolite profiles are presented in Fig. 1.

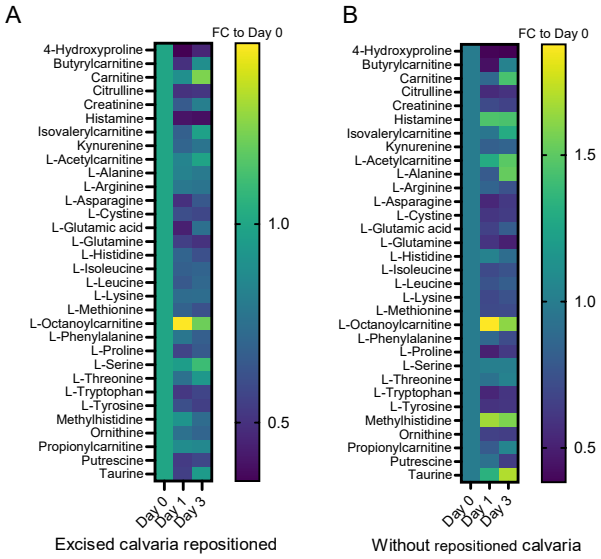

Fig. 1. Serum metabolites of rats with a bone defect: A – with calvarial bone repositioned back to the defect; B – the defect was left empty.

A metabolite analysis of blood samples obtained from the sheep model with a bone defect was performed to confirm the results. For this study, twelve healthy female Swiss white Alpine sheep aged 2–5 years and weighing 60–79 kg underwent pre-enrolment radiological and clinical assessments [10]. After a two-week acclimatization period, serum was collected, and a wedge bone fragment was applied to the tibia. Additional serum samples were taken on days 10, 22, and 29 (post-surgery), followed by euthanasia. Serum samples were further processed using a methanol-based extraction protocol. These

prepared samples were analyzed using LC-MS-based targeted metabolomics, incorporating HILIC-based liquid chromatography, paired with high-resolution mass spectrometric detection. Data processing was conducted using Trace Finder 4.1 software (ThermoScientific). 46 metabolites were detected to evaluate bone healing processes in sheep, as shown in Fig. 2.

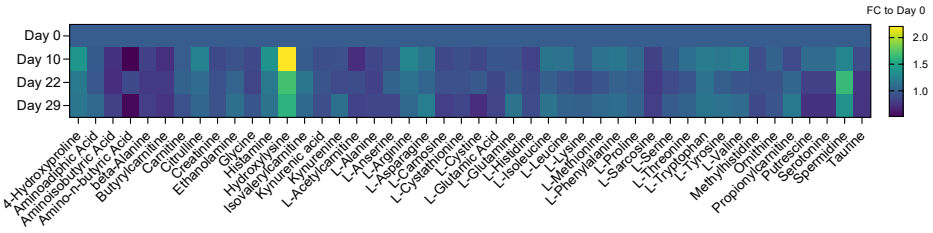

Fig. 2. Serum metabolites of sheep during bone regeneration.

The data analysis of the metabolomics results was performed using MetaboAnalyst 6.0 and GraphPad Prism 9. From analyzing the serum metabolite changes during bone regeneration among both animal models, glutamine and glutamate were the most significantly changed metabolites with a negative relationship to time (Fig. 3 A, C). It is worth noting that glutamine is pivotal as a precursor for glutamate (Fig. 3 B).

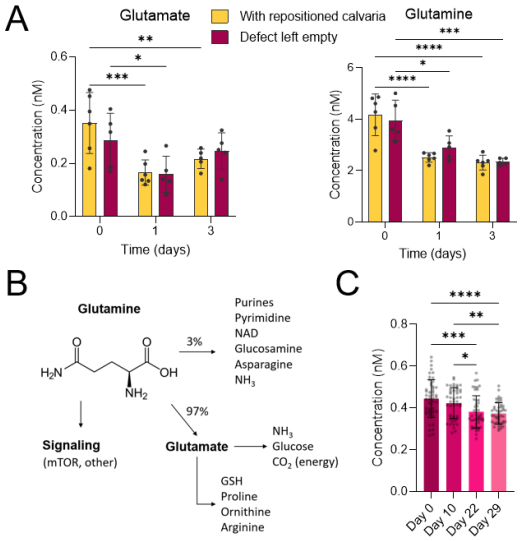

Fig. 3. Metabolomics results indicate a decrease in glutamine and glutamate during bone regeneration among all *in vivo* models. A – Glutamine and glutamate concentrations in rat serum decreased during the regeneration process following a calvarial bone defect, with glutamine showing a more pronounced reduction. The most significant decline of both metabolites occurred on Day 1. B – The glutamine metabolism. Glutamine is primarily metabolized into glutamate [11], [12]. C – The glutamate concentration of sheep serum during bone regeneration showed a gradually decreasing trend. *$p < 0.05$, **$p < 0.01$, ***$p < 0.001$, ****$p < 0.0001$.

The progressive reduction in glutamate concentration during the healing process highlights its significance as an informative biomarker, reflecting the temporal dynamics of bone healing in response to injury. Glutamate is a critical tricarboxylic acid (TCA) cycle carbon source. In hard tissue-relevant microenvironments, glutamate plays a central role in metabolic processes that influence energy production and essential cellular functions, such as biosynthesis, redox regulation, and gene expression [13]. This metabolic pathway is crucial for hard tissue regeneration, emphasizing the importance of glutamine and glutamate as vital nutritional supplements supporting bone healing in cases of bone defects.

Metabolomic investigation of cell-material interaction

The affinity of calcium phosphate (CaP) materials for macromolecules has been extensively studied. However, limited information is available regarding CaP's affinity for metabolites. In this study, the author systematically assessed how CaP influences the metabolic microenvironment, which can, in turn, affect cellular functions. The CaP tablets ($n = 3$) were first immersed in complete culture media (DMEM supplemented with 10 % calf serum (Sigma-Aldrich) and 1 % Penicillin-Streptomycin) for 24 hours; before collection, conditioned medium was removed, and wells were washed with ammonium bicarbonate, then quenched with cold 80 % methanol. The methanol-metabolite solution was collected after 5 minutes of shaking. The samples were then dried using a vacuum centrifuge and reconstituted for LC-MS analysis. Empty wells were used as controls to assess the differences in metabolite adhesion to CaP. To evaluate the impact of adsorption on metabolite levels, the adsorbed metabolites were compared with intracellular metabolite levels. Using Day 1 metabolite concentrations as a reference, 26 metabolites showed a high adsorption rate, with fold changes over 0.1 compared to the cell results (Fig. 4). In general, CaPs showed a lower affinity with the negatively charged amino acids, aspartic acid and glutamic acid. Lactic acid was adsorbed on both the CaP and the control groups, while the lactic acid level on the CaP surface was almost 3 times higher than the control.

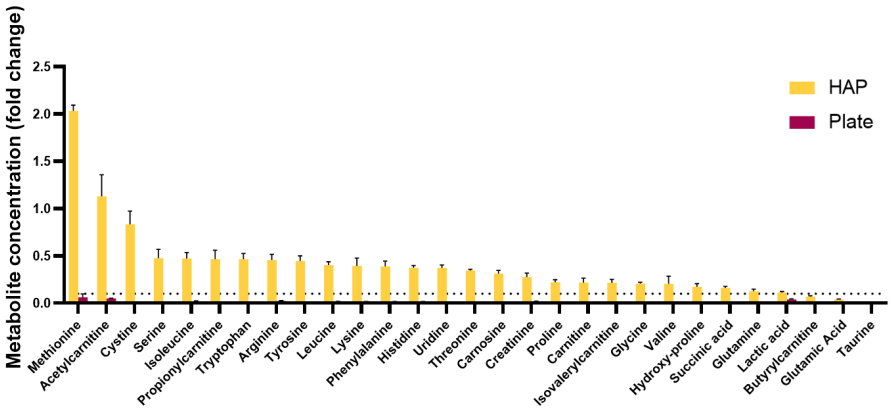

Fig. 4. Metabolites adsorption compared with the cellular metabolite profile. Dashed line: fold change = 0.1.

Although calcium phosphate biomaterials have been widely applied in biomedical engineering, the knowledge of how those materials influence cell metabolism is still missing. The *in vitro* cell metabolomic characterization was used in bioceramics to understand the cellmaterials interaction at a small molecular level. Here, the NIH/3T3 cell line was cultured on CaP tablets. Culture medium was DMEM with 10 % FBS and 1 % P/S, with an initial seeding density of 6×10^4 cells/ml and 1 ml per well/tablet. Cells were washed with ammonium bicarbonate (75 mM, 37 °C) to remove residual metabolites from the culture medium, then quenched in cold 80 % methanol to inhibit enzyme activity. After scraping, the samples were centrifuged. The supernatant was dried by a vacuum centrifuge, and isotopically labeled internal standards were added to the dried samples. Finally, the reconstituted samples were transferred to glass vials for LC-MS analysis. Intracellular metabolites were collected from cells exposed to materials for 1, 3, and 5 days (Fig. 5A). Hydroxyapatite (HAp) and β-tricalcium phosphate (TCP), along with their composites in different ratios – 95 % HAp and 5 % TCP (H95), and 58 % HAp and 42 % TCP (H58) – were used. The composite compositions were selected based on commercial products MBCP® and 4BONE®. The initial exposure to CaPs resulted in a shock pressure on the energy metabolism response to biomaterials, presented by more extensive variability in metabolite profiles. There is a significant difference between the material groups and the control (CNT) among the metabolites involved in energy metabolism (Fig. 5 C). This indicated that the calcium phosphate materials hugely impacted energy production. In the detailed pathway alteration evaluation applied through enrichment analysis (SMPDB), glycolysis stands out as the most influenced pathway (Fig. 5 B), followed by other energy metabolism pathways, which are all included in the top 6. Cells interacting with CaP surfaces displayed increased energy consumption due to heightened glycolysis and TCA cycle activity.

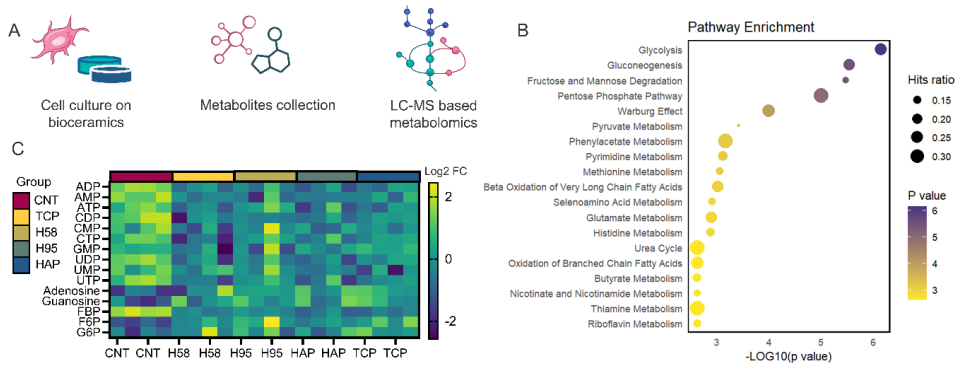

Fig. 5. Metabolomics investigation of cell-materials interaction on calcium phosphate: A – illustration of the experiment procedure; B – pathway enrichment analysis of the intracellular metabolites compared between calcium phosphate materials and the control (metabolomic data from Day 1); C – heatmap of detected metabolites in energy metabolism (metabolomic data from Day 1).

The influence of exposure time and material composition on metabolism

PCA score plots revealed a close clustering of the CaP materials group and a substantial separation between the materials and control groups (Fig. 6). The metabolite changes at the earlier time point presented a more significant variation than the later time points, especially on PC1 (43.1 %), suggesting a more substantial distinction between CaPs and control groups at the initial phase. The amplitude of changes in metabolites gradually becomes smaller. This finding suggests that cells can adjust to the new environment.

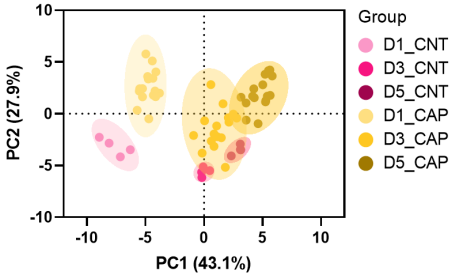

Fig. 6. Cluster analysis by PCA with all CaP and control groups from days 1, 3, and 5 ($n = 4$).

The development of amorphous calcium phosphate with glutamate

Synthesis and manufacture of ACP-Glu

According to the experimental results above, the concept of amorphous calcium phosphate with glutamate (ACP-Glu) was developed. To synthesize ACP with glutamate (ACP-Glu), a 150 mM calcium glutamate solution was prepared in deionized water. Subsequently, the pH of the calcium glutamate solution was carefully adjusted to 11.5 using a 3M NaOH solution. Following the pH adjustment, an equal amount (150 ml) of 100 mM trisodium phosphate solution was added rapidly to

the calcium glutamate solution (total volume 300 ml). Throughout the process, continuous stirring was maintained. Immediately after precipitation, the suspension was centrifuged at 3000 rpm for 5 minutes, and the resulting precipitate was washed three times with deionized water. The precipitate was then frozen by immersing the centrifuge tube in liquid nitrogen for 15 minutes, followed by freeze-drying for 72 hours. The resulting powder was transferred to a 13 mm split-sleeve pressing die (W18Cr4V hardened carbon tool steel, Across International), with tape applied to prevent sticking and contamination. Uniaxial pressure of 1.5 GPa, increasing at approximately 15 MPa/s, was applied using a PW 100 ES electrohydraulic press (P/O/WEBER) and held for 5 minutes before gradual release. The compacted sample was then extracted, with the cold pressing conducted at room temperature (18–25 °C). These pressed tablets were prepared for subsequent in vitro evaluations. For the in vitro evaluations, 0.3 g of each synthesized ACP-Glu was used, while ACP and HAP powders were used as control groups for comparison. The synthesis process and material tablet preparation are illustrated in Fig. 7.

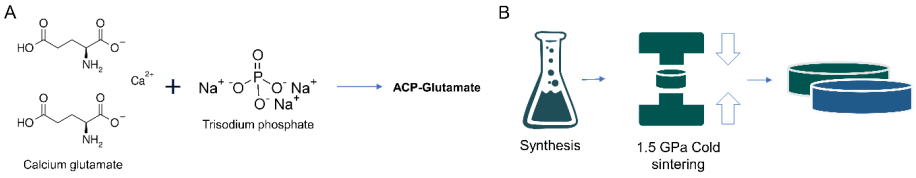

Fig. 7. Material manufacture: A – the synthesis of ACP-Glutamate; B – the preparation of material tablets through cold sintering.

Characterization of ACP-Glu

The prepared ACP-Glu, along with amorphous calcium phosphate (ACP) and hydroxyapatite (HAP), was characterized using scanning electron microscopy (SEM) and X-ray diffraction (XRD). The cold-sintered tablets exhibited a flat surface with particle sizes around 14 nm (Fig. 8 A). The surface morphology and particle sizes of ACP and ACP-Glu were similar. XRD analysis revealed that ACP and ACP-Glu displayed amorphous patterns, while HAP exhibited the characteristic crystalline structure of apatite (Fig. 8 B). The carboxylate ions in glutamate play a role in stabilizing the amorphous phase of ACP [14].

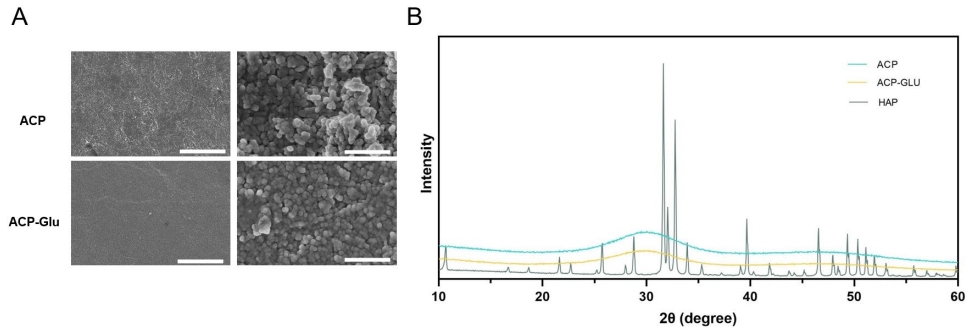

Fig. 8. Characterization of ACP-Glu: A – SEM imaging of ACP and ACP-Glu (scale bar: left 4 μm and right 400 nm); B – XRD pattern of ACP, ACP-Glu, and HAP.

Glutamate release characterization of ACP-Glu

Cold-sintered ACP-Glu tablets (13 mm in diameter, 0.3 g in weight) were submerged in 1 ml of culture medium (DMEM) in a well plate. Conditioned media (50 μl) were collected at 1, 3, 6, 9, 24, 48, and 72 hours post-immersion. 200 μl of methanol was added to each sample to achieve an 80 % methanol proportion. The prepared samples were then analyzed via LC-MS. A line chart illustrates the glutamate release from ACP-Glu in DMEM, with a simple linear regression analysis used to model the release rate (Fig. 9). Both zero-order and first-order models described the cumulative glutamate release well (R^2 = 0.995 and 0.995, respectively). The fitted curves were visually overlapping over 0–72 h, and the two models are statistically hard to distinguish at our sample size. The glutamate release rate was calculated to be approximately 0.01454 nmol (2.14 ng) per hour. This steady, controlled release allows for precise dosage control in bone tissue, helping to achieve the desired therapeutic effect while minimizing potential side effects caused by excessive release.

Unlike surface-coated drug delivery systems, where the active ingredient is external, the glutamate in ACP-Glu is integrated within the material during synthesis. As a result, it exhibits a linear release profile, in contrast to the burst release commonly observed in non-internally loaded materials. Compared to other ACP-based drug delivery systems, which typically show an increasing release trend over time [15], [16], this release from ACP-Glu can match the gradually descending glutamine and glutamate levels from *in vivo* experiments. It is important to note that the experimental setup utilized a stationary environment to mimic in vitro conditions. In real biological scenarios, where various factors such as cell types (e.g., osteoclasts) and dynamic elements like blood flow are present, glutamate's release or uptake rate may differ.

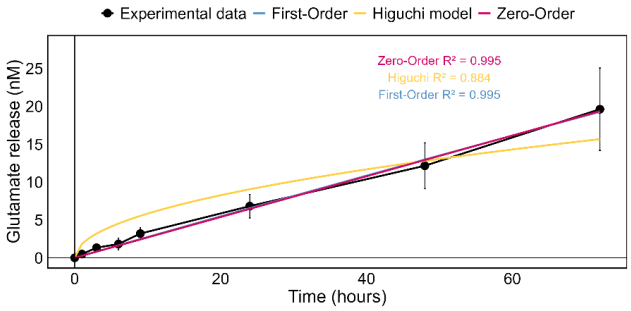

Fig. 9. Glutamate release from ACP-Glu for 72 hours.

Metabolomics investigation of cells on ACP-Glu

MC3T3-E1 preosteoblast-like cell line cultured in DMEM (Gibco) with an extra 50 µg/ml L-ascorbic acid (vitamin C), 10 % FBS (heat-inactivated), and 1 % P/S was applied for metabolomics investigation [17]. The seeding density was 3.5×10^4 cells/ml and 1 ml per well/tablet. The medium recipe of DMEM lacks extra glutamate, which can perfectly mimic the bone injury situation shown in animal studies. Cells were cultured with materials (ACP, ACP-Glu, HAP, and control) for 3 days. On day 3, metabolites were collected by removing the media, washing the cells 3 times with 75 mM ammonium bicarbonate solution, and quenching with cold 80 % methanol. After scraping, the samples were transferred to Eppendorf microtubes and vortexed for 15 seconds. The samples were then centrifuged at 1000 ×g at 0 °C to remove proteins, and the supernatant, containing the metabolites, was collected. The metabolites were dried using a vacuum centrifuge and reconstituted using 80 % methanol and an internal standard. Furtherly targeted quantitative metabolite analysis was conducted using HILIC-based liquid chromatography coupled with mass spectrometric detection on a triple quadrupole mass spectrometer. Statistical analysis was applied through MetaboAnalyst 6.0. For metabolomics data, obtained concentrations were log-transformed and scaled by mean-centering, and each variable was divided by the standard deviation.

Differential metabolite profiles of ACP-Glu and control groups

The volcano plot in Fig. 10 compares the metabolite profiles between ACP-Glu and the control group (CNT, without materials). Two metabolites stand out due to significant alterations: glucose 6-phosphate (FC = 0.20, $p < 0.0001$) and citric acid (FC = 173.20, $p < 0.001$). Glucose 6-phosphate was notably downregulated, while citric acid was significantly upregulated. Glucose 6-phosphate plays a critical role in glucose metabolism, and its downregulation suggests disruptions in energy metabolism or cellular signaling pathways. As the second metabolite in the glycolysis pathway, its reduced levels indicate that the initial steps of glucose metabolism are inhibited. This inhibition could be attributed to enhanced gluconeogenesis, a process supported by the additional availability of glutamate. Citric acid, an important intermediate in the tricarboxylic acid (TCA) cycle, was markedly upregulated. This

increase may point to changes in energy production and the utilization of cellular resources. The significant alterations in these metabolites highlight broader implications for energy metabolism, nucleotide synthesis, neurotransmitter regulation, and cellular signaling processes.

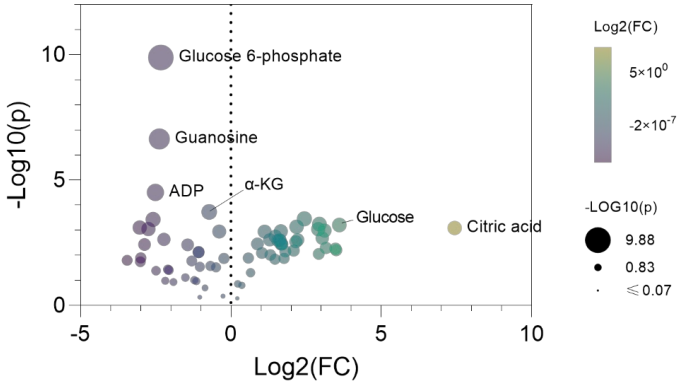

Fig. 10. Volcano plot of metabolites compared between ACP-Glu and CNT. The x-axis is the fold changes, presented as Log2(fold changes); the y-axis is the *p*-value, presented as –Log10(*p*-value).

Metabolite difference between ACP-Glu and ACP

The volcano plot in Fig. 11 compares the metabolites between ACP-Glu and ACP. Citric acid increased 10 times, while malic acid increased 4.4 times from ACP-Glu samples compared with ACP. Consistent with previous assessments, these metabolites are closely associated with energy metabolism, particularly within the TCA cycle. Elevated adenosine levels indicate increased turnover or synthesis of ATP. This could suggest higher energy demands or alterations in ATP utilization or recycling within the cells treated with ACP-Glu. From this result, we can conclude that ACP-Glu has a distinct impact on cellular metabolism, particularly in pathways associated with energy production. The higher levels of TCA cycle intermediates and adenosine in the ACP-Glu group than in the ACP imply potential enhancements or modifications in cellular energy metabolism, possibly leading to increased ATP production or turnover.

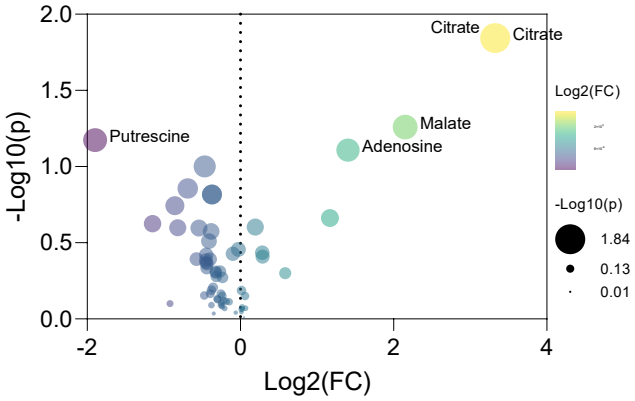

Fig. 11. Volcano plot of metabolites compared between ACP-Glu and ACP. The x-axis is the fold changes, presented as Log2(fold changes); the y-axis is the *p*-value, presented as –Log10(*p*-value).

Focusing on specific metabolites, pre-osteoblasts cultured with ACP-Glu displayed significantly elevated levels of citric acid, approximately 8 times higher than those in the other two CaP groups and about 80 times higher than in the control group (CNT), as shown in Fig. 12 A. Additionally, all CaP groups exhibited higher lactate levels than CNT, though cells treated with ACP-Glu showed lower lactate levels, 0.7 relative to ACP and 0.6 relative to HAP. An enrichment analysis based on the Small Molecule Pathway Database (SMPDB) is presented in Fig. 12 B. The top three enriched pathways – the Warburg effect, acetyl groups into mitochondria, and the TCA cycle – are all associated with energy-producing metabolic processes. The introduction of glutamate appears to induce significant changes in osteoblast metabolism related to energy production. The pathway illustration in Fig. 12 C shows the downregulation of metabolites involved in glycolysis, particularly those related to glucose, the primary sugar substrate. The supplementation of glutamate reduces the reliance on anaerobic glycolysis. Furthermore, the increased anaerobic glycolysis typically induced by CaPs seems to be mitigated by glutamate. Interestingly, metabolites associated with the TCA cycle either remained unchanged or were upregulated, indicating a possible enhancement in TCA cycle activity.

The map also depicts an alternative metabolic route leading to the synthesis of other amino acids. While glutamine experiences a reduction, the levels of two different amino acids, ornithine and proline, remain unaltered. Considering the variations in these metabolic pathways, it becomes evident that the additional glutamate from the substrate actively participates in the TCA cycle.

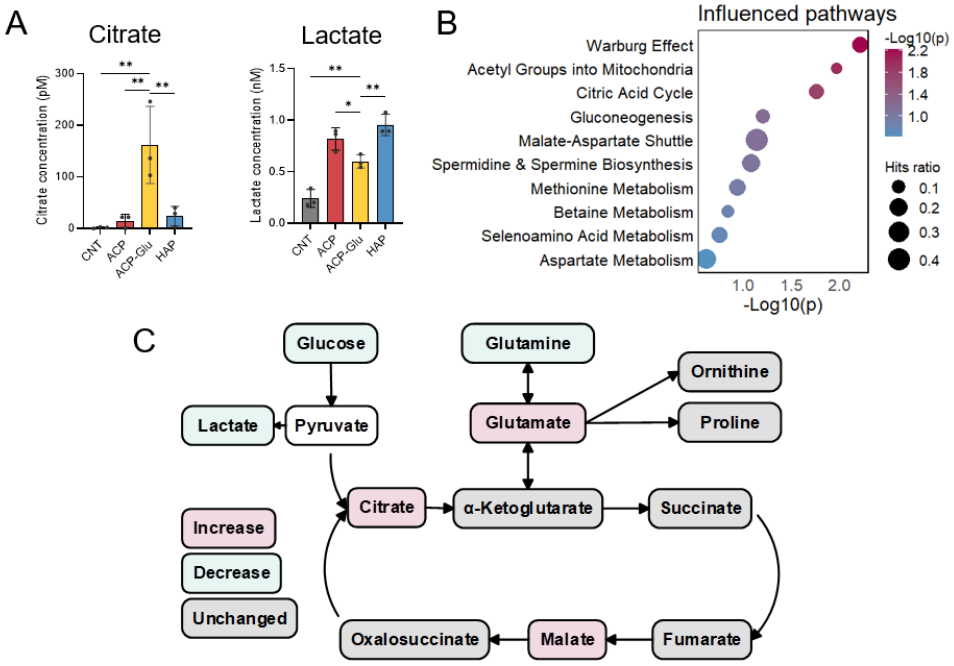

Fig. 12. Energy metabolism pathway alteration: A – the citrate and lactate levels of all groups (*$p < 0.05$, **$p < 0.01$); B – pathway enrichment analysis compared between ACP-Glu and ACP groups; C – metabolism pathway maps are compared between ACP-Glu and ACP (upward arrow means the metabolite level is higher in ACP-Glu, while the downward arrow means the metabolite level is lower in ACP-Glu).

ACP-Glu exhibits a distinct metabolic profile, with citric acid levels approximately 8 times higher than those in the other two CaP groups and about 80 times higher than in the CNT group. The findings indicate significant alterations in key energy-related pathways, including the TCA cycle and glycolysis. Elevated citric acid and malic acid levels suggest increased TCA cycle activity, which may lead to enhanced ATP production or turnover. These metabolic changes highlight the potential of ACP-Glu to influence bone cell behavior, potentially impacting critical processes related to bone health, regeneration, and remodeling.

Osteogenic assessment of ACP-Glu *in vitro*

MC3T3-E1 preosteoblast-like cell line cultured in DMEM (Gibco) with an extra 50 µg/ml L-ascorbic acid (vitamin C), 10 % FBS (heat-inactivated), and 1 % P/S was applied for *in vitro* investigation of osteogenesis [17]. For the biocompatibility test, materials were prepared into small sizes (diameter 6 mm, weight 0.07 g) through cold sintering, and cells were cultured in a 96-well plate with a seeding density of 10,000 cells per well/tablet. The larger-sized material disks were used for the calcium and

phosphate-releasing tests and osteogenesis evaluation (diameter 13 mm, weight 0.3 g). The seeding density was 3.5×10^4 cells/ml and 1 ml per well/tablet. The media recipe of DMEM lacks extra glutamate, which can perfectly mimic the bone injury situation shown in animal studies. The materials used for *in vitro* evaluation were ACP, ACP-Glu, and HAP, while the group without biomaterials was set as a control group.

Biocompatibility test

Cell proliferation was assessed by measuring metabolic activity using the Cell Counting Kit-8 (CCK-8) assay after 24 hours, with cells cultured in DMSO as the positive control group. Cytotoxicity was tested by taking the conditioned cell culture media and presented by LDH assay at 24, 72, and 120 hours after seeding the cells (Fig. 13). The cell viability assessment using CCK-8 indicated that ACP-Glu exhibited higher cell viability compared to both the control ($p = 0.0102$) and HAP ($p = 0.0166$), with no significant difference observed between ACP and ACP-Glu ($p = 0.5150$). The presence of glutamate in ACP-Glu could play a role in promoting cell viability. Glutamate is an amino acid involved in various cellular processes, including energy production and protein synthesis. It provides additional nutrients or supports the metabolic activities of the cells, leading to higher cell viability [18]. The lower cell viability observed without glutamate suggests that this amino acid is essential for energy metabolism, protein synthesis, and neurotransmission. A deficiency in glutamate can impair these processes, resulting in reduced cell viability. The lactate dehydrogenase (LDH) assay, which measures the release of LDH – an enzyme released when cell membranes are damaged – showed no toxicity across all groups. Although differences in cell viability were observed in terms of proliferation, the release of glutamate did not cause damage to cell structures or lead to cell death.

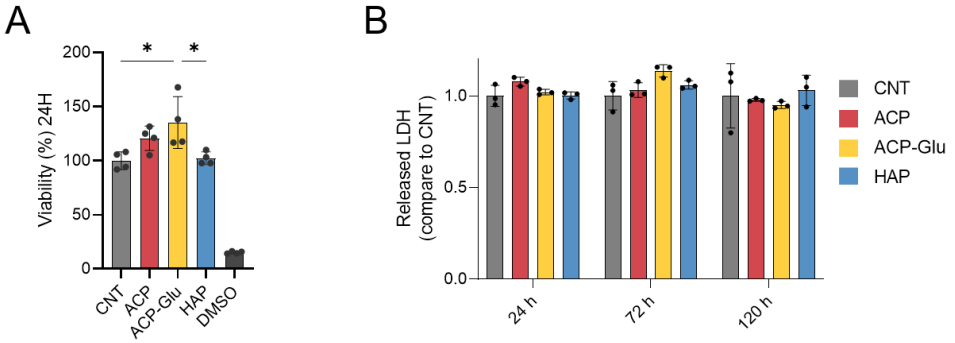

Fig. 13. A – Cell proliferation of MC3T3-E1 cultured after 24 hours ($n = 4$), *$p < 0.05$. B – Released LDH levels of all groups after culturing 24, 72, and 120 hours ($n = 3$).

Extracellular and intracellular calcium and phosphate levels

As described earlier, calcium and phosphate levels in the conditioned culture media were measured on days 10 and 14 after cell seeding. The calcium level in the medium was measured by a calcium

colorimetric assay kit (Sigma), and the phosphate level in the medium was measured by a phosphate assay kit (Sigma). One-way ANOVA followed by a post hoc Tukey test was used to detect group differences. Both ACP and ACP-Glu demonstrated enhanced calcium ion release, even in the presence of pre-existing calcium ions in the culture medium (Fig. 14 A). Notably, the conditioned media from ACP-Glu contained significantly higher calcium ion levels, 2.2 times greater than ACP and 1.9 times greater than HAP on day 14, suggesting that the amorphous crystals dissolve faster than hydroxyapatite. Osteoblasts near the material can take up these calcium ions from the medium, which can then be used for bone mineralization and other cellular processes [19]. Amorphous calcium phosphate has higher solubility compared to HAP [20]. This means ACP readily dissolves in aqueous solutions, including culture media, releasing calcium and phosphate ions into the surrounding liquid – the lack of a defined crystal structure in ACP results in faster dissolution kinetics. This is because the disordered structure of ACP allows water molecules to penetrate more efficiently, leading to quicker breakdown and release of calcium and phosphate ions [21]. This makes the difference in the solubility of ACP under different environments (temperature, pH).

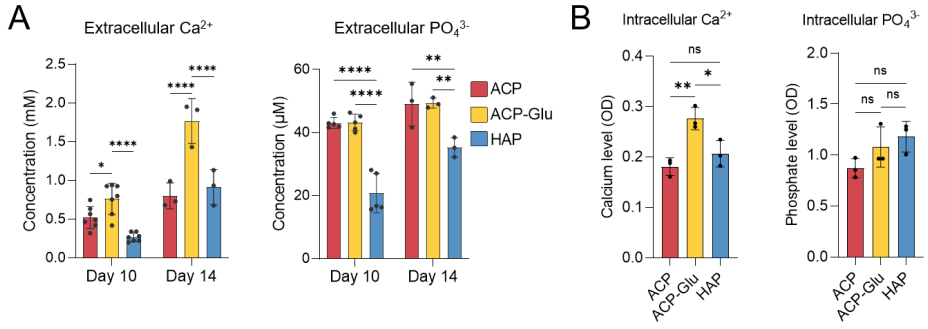

Fig. 14. A – Calcium and phosphate levels in the media on day 10 and day 14. B – Intracellular calcium and phosphate levels on day 14, presented by OD.

Intracellular calcium and phosphate levels were quantified on day 14 in triplicate for each group, as shown in Fig. 14 B. After removing the culture media, the cells were washed twice with PBS. Tris-HCl containing 1 % Triton X-100 was used to lyse the cells, and the collected samples were transferred into Eppendorf microtubes and vortexed for 15 seconds. Ion levels were then measured using a calcium colorimetric assay kit (Sigma) and a phosphate assay kit (Sigma) on a 96-well plate. The results showed that HAP and ACP-Glu promoted higher intracellular calcium levels than ACP. However, the groups had no significant differences in intracellular phosphate levels. ACP-Glu creates a high-calcium environment that enhances calcium uptake by cells, with glutamate possibly influencing calcium metabolism. This may affect calcium signaling and cellular responses, improving calcium uptake in cells [22]. Notably, the data is from only one time point, which is already after 14 days of culture. There

may be unknown influences from many other factors during this period, such as calcium and phosphorus deposits caused by parts mineralized on the CaP tablets.

Osteogenesis evaluation

An alkaline phosphatase (ALP) assay was performed using p-nitrophenyl phosphate tablets (Sigma) to evaluate the initial stages of osteogenesis in cells cultured on CNT, ACP, ACP-Glu, and HAP. ALP activity was measured by quantifying the formation of p-nitrophenol from p-nitrophenyl phosphate. ALP plays a crucial role in mineralizing the extracellular matrix in bone tissue. As pre-osteoblasts mature into osteoblasts, they synthesize the bone matrix, which includes collagen and other proteins. ALP facilitates matrix mineralization by dephosphorylating compounds like inorganic pyrophosphate, a mineralization inhibitor. The ALP level at the initial point in time is similar (Fig. 15 A). ALP level of ACP-Glu showed a significantly higher level at later points. As an osteogenic marker, ALP reflects early osteoblast differentiation and the progression of osteogenesis. These results suggest that the ACP-Glu ceramic tablet promotes better osteogenic differentiation than the control, ACP, and HAP.

Osteopontin (OPN) and osteocalcin (OCN) levels were measured in the culture medium on days 7 and 14 to assess osteogenic signaling markers further. OPN levels were evaluated using the Mouse Osteopontin ELISA Kit (RAB0437) from Sigma, and OCN levels were assessed using the Mouse Osteocalcin ELISA Kit (ab285236) from Abcam. The ACP-Glu group exhibited significantly higher OPN levels at both time points. On day 7, ACP-Glu showed no significant difference from ACP and HAP but displayed a notably higher level than the control group (Fig. 15 B). OPN is an intrinsically disordered protein featuring a notable negative charge, with approximately 25 % of the protein's composition comprising aspartate or glutamate residues [23]. As the supplier of one of the significant compositions of this protein, ACP-Glu may contribute to the manufacture of OPN as well.

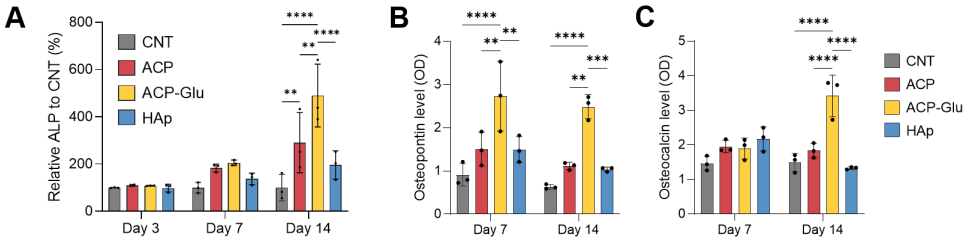

Fig. 15. Osteogenesis marker level: A – ALP level compared to CNT; B – OPN level; and C – OCN level.

The OCN level on day 7 showed a similar pattern across all groups. OCN, a marker of mature osteoblasts involved in bone matrix production, indicated that the cells in all groups were at a relatively early stage of osteoblast differentiation on day 7 (Fig. 15 C). The effects of the presence or absence of glutamate became apparent on day 14. The OCN level in cells cultured on ACP-Glu was 1.86 times higher than that in the ACP group and 2.57 times higher than that in the HAP group. This suggests that

the cells in the ACP-Glu group had advanced further in their differentiation and maturation by day 14. The presence of glutamate in the ACP-Glu group likely enhanced osteoblast activity and accelerated differentiation. The significant increase in OCN level over time indicates that the differentiation process in the ACP-Glu group may be progressing more rapidly than the other groups at both time points.

Mineralization evaluation

Alizarin Red staining is commonly used to detect and quantify calcium deposits, indicating mineralization in biomaterials. This dye binds to calcium ions, producing a red color that can be visualized and quantified using microscopy or spectrophotometry, aiding in the characterization of osteogenic differentiation and mineralization in tissue-engineered constructs. An indirect culture method was applied to prevent direct staining of the materials themselves. The materials, in powder form, were placed on a transwell insert above the cultured cells (as indicated in Fig. 16 A). MC3T3-E1 cells were seeded in a 6-well plate at a density of 3.5×10^4 cells/ml and 3 ml in each well, cultured under non-glutamate media (DMEM as described at the beginning of this chapter) for 21 days in triplicate. Pure ACP material was applied as the control group. The results revealed distinct mineralization patterns across the experimental groups, as assessed by Alizarin Red staining. After 21 days of culture, the media was removed, and the wells were gently washed three times with deionized water. Subsequently, 1 ml of Alizarin Red solution was added to each well for 1 minute, followed by five washes with deionized water. The ACP-Glu groups exhibited better mineralization results (Fig. 16 B). Macroscale images showed a more intense red staining on the well-plate surfaces in the ACP-Glu groups. Under optical microscopy, more extensive mineralized deposits were observed in the ACP-Glu groups than in other groups. Although material penetration through the transwell filter may have affected the experiment's precision, the results were still significant when comparing both calcium phosphate (CaP) materials. Not only the calcium but also the glutamate released from the materials contribute to the osteogenesis of osteoblasts. The absence of glutamate appeared to limit osteoblast mineralization, while the presence of glutamate-containing materials enhanced the primary function of osteoblasts in forming new bone structures. These findings further demonstrate the superior osteogenic induction capabilities of ACP-Glu in promoting mineralization and bone formation.

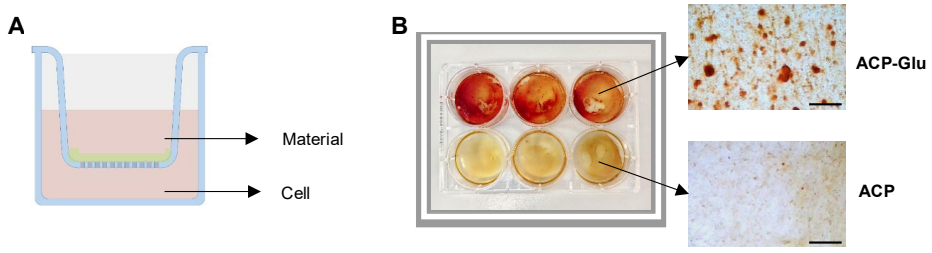

Fig. 16. Alizarin Red staining: A – illustration of indirect cell culture with materials; B – the overall view after a camera and the microscope captured Alizarin Red staining. ACP-Glu is up, and ACP is down in the figure. Scale bar = 30μm.

Conclusions

1. Critical-size bone defects lead to significant metabolic fluctuations, notably depleting nutritional metabolites and reducing glutamine and glutamate.
2. Calcium phosphates (CaPs) adsorb low molecular metabolites, particularly amino acids, and influence cellular amino acid and energy metabolism pathways.
3. Anaerobic metabolism increases when cells come into contact with CAPs, especially on day 1.
4. Amorphous calcium phosphate (ACP) with glutamate (ACP-Glu) demonstrates controlled and gradual release of glutamate in 3 days, which is critical for supporting cellular functions during tissue repair.
5. Cold-sintered ACP-Glu outperforms hydroxyapatite and ACP in promoting cellular mineralization processes, with 2 times higher OCN and OPN levels and more prominent Alizarin Red staining results.
6. ACP-Glu changes energy metabolism, particularly enhancing the tricarboxylic acid cycle post-gluconeogenesis. Exposure to ACP-Glu resulted in an 8 times higher intracellular citric acid level than other investigated CAPs.

References

1. Wu, A. M., Bisignano, C., James, S. L., Abady, G. G., Abedi, A., Abu-Gharbieh, E., et al. Global, regional, and national burden of bone fractures in 204 countries and territories, 1990–2019: a systematic analysis from the Global Burden of Disease Study 2019. The Lancet Healthy Longevity. 2021; 2(9): e580–592.

2. Yousefi, A. M. A review of calcium phosphate cements and acrylic bone cements as injectable materials for bone repair and implant fixation. Journal of Applied Biomaterials and Functional Materials. 2019; 17(4).

3. Pandit, A., Indurkar, A., Locs, J., Haugen, H. J., Loca, D. Calcium Phosphates: A Key to Next-Generation In Vitro Bone Modeling. Advanced Healthcare Materials. 2024.

4. Galotta, A., Sglavo, V. M. The cold sintering process: A review on processing features, densification mechanisms and perspectives. Journal of the European Ceramic Society. 2021; 41(16): 1–17.

5. Choi, I. A., Umemoto, A., Mizuno, M., Park-Min, K. H. Bone metabolism – an underappreciated player. npj Metabolic Health and Disease. 2024; 2(1): 1–10.

6. Xia, D., Wu, R., Xue, Q., Jiang, G., Xu, S. Metabolomics provides insights into acceleration of bone healing in fractured patients with traumatic brain injuries. Biomedical Chromatography. 2023; 37(11).

7. Zhang, X., Xu, H., Li, G. H. Y., Long, M. T., Cheung, C., Vasan, R. S., et al. Metabolomics insights into osteoporosis through association with bone mineral density. Journal of Bone and Mineral Research. 2021; 00(00): 1–10.

8. Lv, D., Zou, Y., Zeng, Z., Yao, H., Ding, S., Bian, Y., et al. Comprehensive metabolomic profiling of osteosarcoma based on UHPLC-HRMS. Metabolomics. 2020; 16(12): 1–11.

9. Fan, J., Jahed, V., Klavins, K. Metabolomics in bone research. Metabolites. 2021; 11(7).

10. Barcik, J., Ernst, M., Buchholz, T., Constant, C., Mys, K., Epari, D. R., et al. The absence of immediate stimulation delays bone healing. Bone. 2023; 175(April): 116834.

11. Watford, M. Glutamine and glutamate: Nonessential or essential amino acids? Animal Nutrition. 2015; 1(3): 119–122.

12. Timblin, G. A., Tharp, K. M., Ford, B., Winchester, J. M., Wang, J., Zhu, S., et al. Mitohormesis reprogrammes macrophage metabolism to enforce tolerance. Nature Metabolism. 2021; 3(5): 618–635.

13. Shang, M., Cappellesso, F., Amorim, R., Serneels, J., Virga, F., Eelen, G., et al. Glutamine Metabolism Controls Chondrocyte Identity and Function. Developmental Cell. 2020; 53(5): 530–544.e8.

14. Indurkar, A., Choudhary, R., Rubenis, K., Nimbalkar, M., Sarakovskis, A., Boccaccini, A.R., et al. Amorphous Calcium Phosphate and Amorphous Calcium Phosphate Carboxylate: Synthesis and Characterization. ACS Omega. 2023; 8(30): 26782–26792.

15. Visan, A. I., Ristoscu, C., Popescu-Pelin, G., Sopronyi, M., Matei, C. E., Socol, G., et al. Composite drug delivery system based on amorphous calcium phosphate–chitosan: An efficient antimicrobial platform for extended release of tetracycline. Pharmaceutics. 2021; 13(10).

16. Sun, R., Åhlén, M., Tai, C. W., Bajnóczi, É. G., de Kleijne, F., Ferraz, N., et al. Highly porous amorphous calcium phosphate for drug delivery and bio-medical applications. Nanomaterials. 2020; 10(1): 1–18.

17. Izumiya, M., Haniu, M., Ueda, K., Ishida, H., Ma, C., Ideta, H., et al. Evaluation of mc3t3-e1 cell osteogenesis in different cell culture media. International Journal of Molecular Sciences. 2021; 22(14): 1–12.

18. Walker, M. C., van der Donk, W. A. The many roles of glutamate in metabolism. Journal of Industrial Microbiology and Biotechnology. 2016; 43(2–3): 419–430.

19. Salhotra, A., Shah, H. N., Levi, B., Longaker, M. T. Mechanisms of bone development and repair. Nature Reviews Molecular Cell Biology. 2020; 21(11): 696–711.

20. Luginina, M., Orru, R., Cao, G., Luginina, M., Grossin, D., Brouillet, F., et al. First successful stabilization of consolidated amorphous calcium phosphate (ACP) by cold sintering: Toward highly-resorbable reactive bioceramics. Journal of Materials Chemistry B. 2020; 8(4): 629–635.

21. Degli Esposti, L., Iafisco, M. Amorphous calcium phosphate, the lack of order is an abundance of possibilities. Biomaterials and Biosystems. 2022; 5(December 2021): 100037.

22. Pei, Z., Lee, K. C., Khan, A., Erisnor, G., Wang, H. Y. Pathway analysis of glutamate-mediated, calcium-related signaling in glioma progression. Biochemical Pharmacology. 2020; 176.

23. Kariya, Y., Kariya, Y. Osteopontin in Cancer: Mechanisms and Therapeutic Targets. International Journal of Translational Medicine. 2022; 2(3): 419–447.

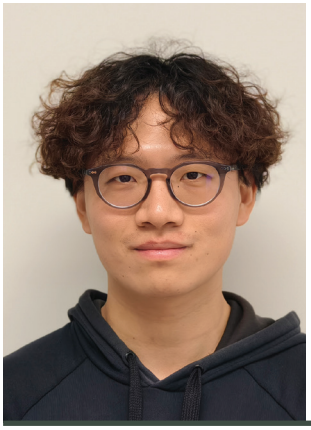

Jingzhi Fan was born in 1995 in Liaoning, China. He obtained his Bachelor's degree in Biomaterials (2018) from Beijing University of Chemical Technology and a Master's degree in Materials Science and Engineering (2019) from University College Dublin. Since 2020, he has been a PhD student at Riga Technical University. In 2021, he was a visiting researcher at AO Research Institute Davos. He is currently a research assistant at Riga Technical University. His research interests are biomedical engineering and metabolism.